Neuroanatomical foundations of social tolerance across macaque species

S. Silvère[1,2], J. Lamy[3], C. Po[3], M. Legrand[1,2], J. Sallet[4,5], S. Ballesta[1,2]

1. Laboratoire de Neurosciences Cognitives et Adaptatives, UMR 7364, Strasbourg, France

2. Centre de Primatologie de l'Université de Strasbourg, Niederhausbergen, France

3. ICube (UMR 7357), Université de Strasbourg-CNRS, Strasbourg, France

4. Univ Lyon, Université Lyon, Inserm, Stem Cell and Brain Research Institute, U1208, Bron, France

5. Wellcome Center for Neuroimaging, Dpt of Experimental Psychology, University of Oxford, Oxford, UK.

Abstract

The macaque genus includes 25 species with hugely diverse social systems, ranging from low to high tolerance social organization. Such interspecific behavioral variability provides a unique model to tackle the evolutionary foundation of primate social brain. Yet, the neuroanatomical correlates of these social tolerance grades remain unknown. To address this question, we analyzed *post-mortem* structural scans from 12 macaque species. Our results show that amygdala volume is a subcortical predictor of macaques' social tolerance, with high tolerance species exhibiting larger amygdala than low tolerance ones. To tackle the issue of nature versus nurture origin of the social tolerance effect on amygdala volume, we investigated the development of amygdala across species with different social grades. Intolerant species showed a gradual increase in relative amygdala volume across the lifespan. Unexpectedly, tolerant species exhibited an opposite trend, previously undescribed in primates. Taken together, these findings provide valuable insights into the neuroanatomical and evolutionary basis of primates' social behaviors.

Keywords: non-human primate, social tolerance, social brain, amygdala, MRI, comparative neuroanatomy

Introduction

Complex social environment implies a greater cognitive demand of social representations and interactions, which is one of the driving forces behind the evolution of the primate brain (Dunbar, 2009; Heldstab et al., 2022) . Correlations between social environment and variations in brain structures volumes have been reported, both in humans (Kanai et al., 2012; Maguire et al., 2000; Parkinson et al., 2017) and in NHP (Noonan et al., 2014a; Sallet et al., 2011; Meguerditchian et al., 2021; Testard et al., 2022). Previous studies have established, within single species, correlation of social characteristics such as the hierarchical status of an individual (Noonan et al., 2014b; Testard et al., 2022) or the group size (Meguerditchian et al., 2021; Sallet et al., 2011; Testard et al., 2022), with grey matter volumes in the amygdala, the hippocampus, the superior temporal sulcus (STS) and the rostral prefrontal cortex (rPFC) in rhesus macaque (*M. mulatta)* (Meguerditchian et al., 2021; Sallet et al., 2011; Testard et al., 2022).

Despite the existence of 25 species within the *Macaca* genus (Cooper et al., 2022; Cords, 2012; Ghosh et al., 2022; Thierry, 2007; Thierry et al., 2004), most neuroscience research focuses on two species, *M. mulatta* and *M. fascicularis* (and in rare cases *M. nemestrina* and *M. fuscata* (Carlo et al., 2010; Isa et al., 2009; Maranesi et al., 2014)). Although the evolutionary divergence time within this genus is relatively short (6 to 8 million years (Perelman et al., 2011)), the various macaque species display a considerable interspecific variety of social behaviors while usually maintaining a multi-male, multi-female, and multi-generational social structure (Balasubramaniam et al., 2018; Thierry, 2007, 2000). These behavioral differences are characterized by different styles of dominance (Balasubramaniam et al., 2012), severity of agonistic interactions (Duboscq et al., 2014), nepotism (Berman and Thierry, 2010; Duboscq et al., 2013; Sueur et al., 2011) and submission signals (De Waal and Luttrell, 1985; Rincon et al., 2023), among the 18 covariant behavioral traits described in Thierry's classification of social tolerance (Thierry, 2021, 2017, 2000). Thus, species classified as grade 1 in social tolerance (i.e. *M. mulatta*), indicative of low social tolerance, are prone to violent conflicts with an average reconciliation rate of less than 20% (Thierry, 2007, 2000). Typically, aggression is directed mainly at lower-ranking, unrelated individuals, who are expected to flee or submit to the attacker (Thierry, 2007, 2000). Conversely, species classified in social tolerance grade 4, which exhibit high social tolerance, are less prone to violent conflict, which is often bidirectional and characterized by more frequent protests and counter-attacks by lower-ranking individuals (Thierry, 2007, 2000). In addition, they tend to have a higher reconciliation rate, reaching up to 50% (Thierry, 2007, 2000). Despite these differences macaque species display similar general cognition skills (ManyPrimates et al., 2022), with

differences in cognitive abilities (such as inhibitory control) being thought to be associated with constraints specific to social interactions defined by social tolerance grade of each species (Joly et al., 2017; Loyant et al., 2023). Altogether the specific socio-behavioral diversity of macaques' species represents an important model for investigating the evolution of social cognition and its impacts on neural circuits.

Taken advantage of databases of magnetic resonance imaging (MRI) structural scans, we conducted the first comparative study integrating neuroanatomical data and social behavioral data from closely related primate species of the same genus to address the following questions: To what extent can differences in volumes of subcortical brain structures be correlated with varying degrees of social tolerance? Additionally, we tested whether these dispositions reflect primarily innate features, shaped by evolutionary processes, or acquired through socialization within more or less tolerant social environments. To achieve these goals, we needed to propose a conceptual framework for analyzing differences in social tolerance across macaque species in terms of cognitive domains that could be linked to neuroanatomical variations. We thus categorized the 18 behavioral traits tolerance grades (Thierry et al., 2000), into three cognitive categories: "socio-cognitive demands," "social predictability," and "inhibitory control". We thought to capture with these three cognitive domains the mains behavioral differences between intolerant and socially tolerant species. For example, macaques with high social tolerance, such as Tonkean macaques (*M. tonkeana*), have much denser social networks due to their more relaxed hierarchy (Balasubramaniam et al., 2018; Sueur et al., 2011). Thus, individuals in socially tolerant groups tend to interact more freely, with less regard for hierarchy compared to intolerant species. It suggests that these grade 4 species face more frequent and diverse cognitive demands from their social environment than grade 1 species. We associated these three categories with neuroanatomical hypotheses regarding variations in the volume of two subcortical structures of interest, the amygdala and the hippocampus. Based on existing literature on the effects of the social environment and stress on the volume of these two regions and their implication in social cognition (Bickart et al., 2011; Caetano et al., 2021; Coplan et al., 2014; Dark et al., 2021; Haley et al., 2012; Howell et al., 2014; Lyons et al., 2001; Sallet et al., 2011), we hypothesized that increased cognitive demands from the social environment could lead to a differential effect on amygdala and hippocampus volumes (Bickart et al., 2011; Haley et al., 2012; Lyons et al., 2001; Sallet et al., 2011). We summarized our hypotheses into a table comparing grade 4 and grade 1 species (**Table 1**).

Table 1: Subcortical neuroanatomical hypotheses

Cognitive requirements (4 vs 1)	Related behavioral traits (4 vs 1)	Neuroanatomical correlates (4 vs 1)
Higher Socio-cognitive demands	Denser social network[1] More complex communicative skills[2] Development of cooperative behaviors Higher rate of reconciliation	Amygdala volume higher[3] Hippocampus volume higher[4]
Less predictable social environment[5]	Lower degree of dominance asymmetry Lower nepotism Higher rate of affiliative contact	Amygdala volume higher[6] Hippocampus volume lower[7]
Better inhibitory control (Less impulsivity, Less aggressivity[8])	More intense aggression Higher rate of reconciliation	Amygdala volume lower[9] Hippocampus volume stable[10]

Summary table of our hypotheses highlighting the behavioral differences between grades 1 and 4 and their cognitive and neuroanatomical implications for the amygdala and hippocampus. Behavioral traits are based on Thierry, 2021. Other studies that support our theoretical framework are cited in the table.

We tested our hypothesis using 42 *post-mortem* MRI acquisitions of 12 macaque species representing the four grades of social tolerance. The dataset was composed of samples from open access databases (Milham et al., 2018; Navarrete et al., 2018; Sakai et al., 2018) as well as newly and unpublished samples from the collection of the Centre de Primatologie de l'Université de Strasbourg (CdP) and INSERM-Oxford University. These samples include brain images of *M. tonkeana* and *M. thibetana,* two macaque species that have never been scanned before as well as scan of *M. nigra* that is rare in the existing literature (Navarrete et al., 2018; Sakai et al., 2023). We show, to the best of our knowledge, the first neuroanatomical

[1] (Balasubramaniam et al., 2018; Sueur et al., 2011)
[2] (Rebout et al., 2022, 2020)
[3] (Bickart et al., 2011; Sallet et al., 2011; Testard et al., 2022)
[4] (Kanai et al., 2012; Testard et al., 2022; Todorov et al., 2019)
[5] (Sadoughi et al., 2021; Vandeleest et al., 2016)
[6] (Bickart et al., 2011; Sallet et al., 2011; Testard et al., 2022; Tottenham and Sheridan, 2010)
[7] (Kim et al., 2015; Lyons et al., 2001; Meyer and Hamel, 2014)
[8] (Joly et al., 2017; Loyant et al., 2023)
[9] (Testard et al., 2022; Tottenham and Sheridan, 2010)
[10] (Tottenham and Sheridan, 2010)

correlates of the social tolerance grade of the *Macaca* genus. In fact, the amygdala's volume was found to be significantly correlated with the social tolerance grade between the different macaque species; furthermore, our findings corroborate the established correlation between the relative growth of the amygdala in primates. However, we identify an inverse relationship in the most tolerant species of macaque monkeys. This study offers a novel and valuable perspective by comparing inter-species brain structures to investigate the functioning of the social brain, while accounting for key socio-cognitive variables.

Results

We obtained structural MRI scans of 42 macaques of 12 macaque species. Using a semi-automated registration to an atlas (SARM (Hartig et al., 2021)), we extracted amygdala and hippocampus volumes and analyzed whether these covaried with social grade and age, using a Bayesian model. The amygdala's volume, the main response variable, showed a strong dependence on total volume, but no discernible patterns with other individual predictors when visualized by scatterplots (**Figure 2**).

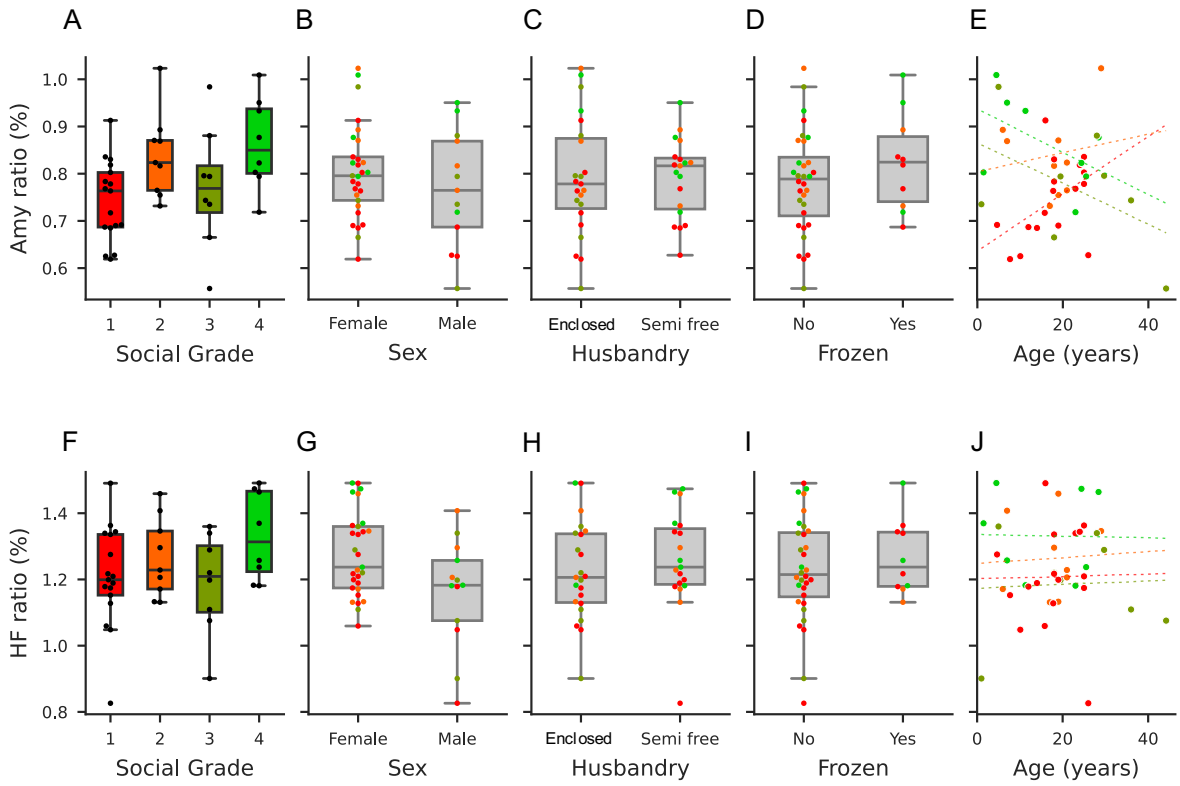

Figure 2: Model predictors of the amygdala and hippocampus, and volume predictions across social tolerance grades. *First row* ***(A–D)****: Model predictors and responses for amygdala volume. The volume ratio is calculated as the amygdala volume divided by the total brain volume (excluding the myelencephalon and cerebellum).* ***(A)*** *Distribution of amygdala volume ratios across social tolerance grades.* ***(B)*** *Distribution of amygdala volume ratios by sex.* ***(C)*** *Distribution of amygdala volume ratios by husbandry condition (enclosed vs. semi-free).* ***(D)*** *Distribution of amygdala volume ratios by the frozen status.* ***(E)*** *Distribution of amygdala volume ratios by age. Second row* ***(F–J)****: Model predictors and responses for hippocampal volume. The volume ratio is calculated as the hippocampal volume divided by the total brain volume (excluding the myelencephalon and cerebellum).* ***(F)*** *Distribution of hippocampal volume ratios across social tolerance grades.* ***(G)*** *Distribution of hippocampal volume ratios by sex.* ***(H)*** *Distribution of hippocampal volume ratios by husbandry condition (enclosed vs. semi-free).* ***(I)*** *Distribution of hippocampal volume ratios by the frozen status.* ***(I)*** *Distribution of hippocampal volume ratios by age.*

Model quality and coefficients

The R^2 coefficient of determination of the model indicated a large proportion of variability accounted for by the model (90% credible interval: [0.87, 0.97]). The effect of sex was minimal for the amygdala but more pronounced for the hippocampus (**Figure 3**), whereas husbandry had a limited effect on both regions of interest. Amygdala volume increased with social grade (independently of its interaction with age) and with age (independently of its interaction with social grade). However, the interaction between social grade and age suggested that the trajectory of amygdala volume over the lifespan differs across social grades, as detailed below. In contrast, hippocampal volume remained relatively stable across social grades and ages. Despite limited sample size, the interaction between social grade and age suggested a differential trajectory of amygdala volume across the lifespan among different social grades (**Figure 3**).

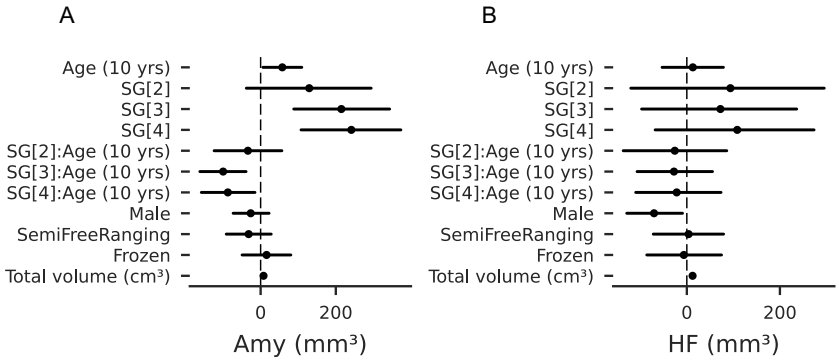

Figure 3: Parameters of the model. (A) *Parameters of the model for the amygdala volume.* ***(B)*** *Parameters of the model for the hippocampal volume. SG [x]: Social Grade [x] vs Social Grade [1]; SG[x]:Age (10 years): Social Grade-Age interaction.*

Predicted data

Figure 4 illustrates how amygdala's volume development varies with an individual's social grade over their lifespan. Two results stand out: first, individuals in Social Grade 1 showed a distinct pattern of amygdala volume development compared to other social grades. Although Grade 1 individuals had a smaller amygdala volume in early years compared to the other Social Grades, the amygdala's volume variation slope was steeper than for the other Grades (slope with 90% credible intervals [0.6, 11.0]). This increase contrasted with trends observed in Grades 3 (slope with 90% CI [-7.6, -0.9]) and 4 (slope with 90% CI [-8.0, 1.9]), which showed a decrease in volume over time. Individuals in Grade 2 also showed a slight increase in amygdala volume (slope with 90% CI [-4.4, 9.3]), similar to grade 1 but not as steep.

When comparing Grade 1 and Grade 4, individuals in Grade 4 showed larger amygdala volumes until approximately 26 years of age. After this age the trend reversed, with Grade 1 individuals showing relatively larger amygdala volumes in later life. From 0 to 24 years old,

Grade 2 individuals had larger amygdala volumes than grade 1 individual. However, this trend reversed after the age of 24, so that older Grade 2 individuals had smaller amygdala volumes than Grade 1 individuals.

The comparison between Grade 2 and Grade 3 showed that the volumes were not consistent, as Grade 2 shows a slight upward trend over time, whereas Grade 3 showed a decrease. In addition, individuals in Grade 4 consistently showed slightly larger amygdala volumes compared to those in Grade 3. Finally, as expected from the model parameters, hippocampal volume showed minimal variation over time, with Grade 1 species showing a small increase in hippocampal volume over their lifetime compared to the other social grades.

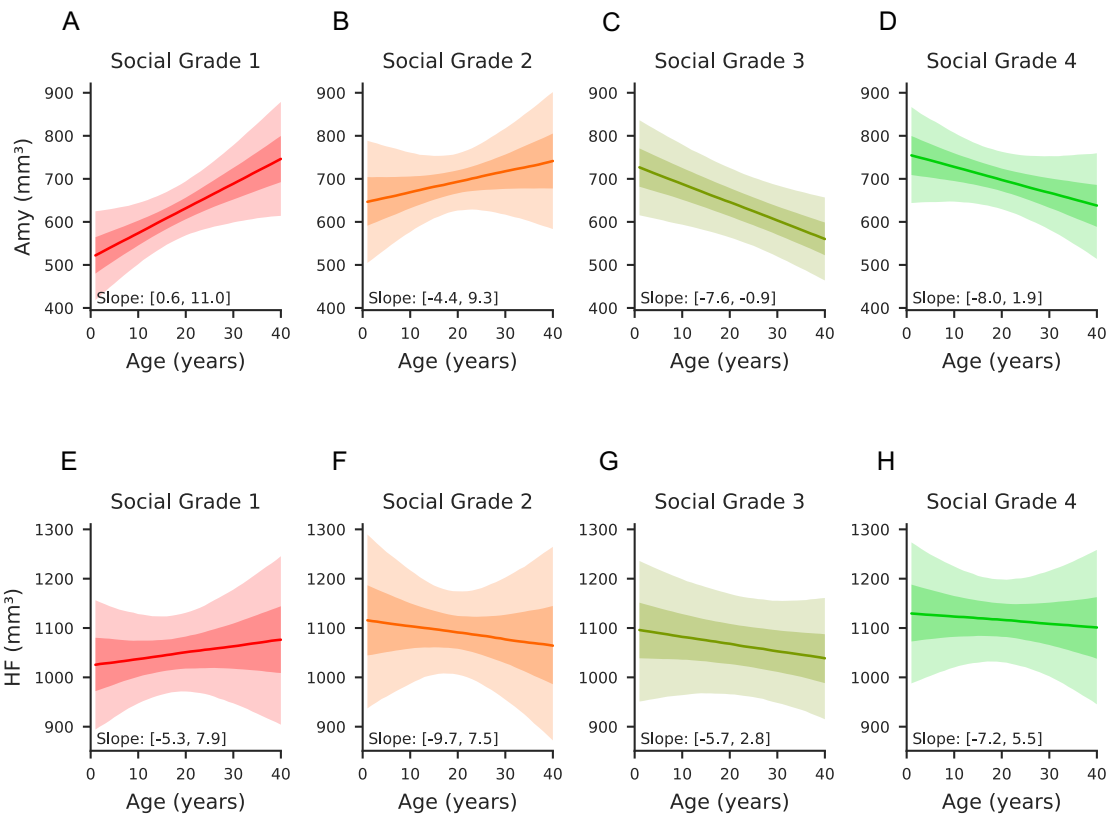

Figure 4: Volume predictions across social tolerance grades of the amygdala and hippocampus. *All panels represent the predictions of the multivariate Bayesian linear model, where all the variables are kept constant (including total brain volumes) in order to represent the effect of age only on the volume of amygdala and hippocampus. First row* ***(A–D)****: Predicted amygdala volume across social tolerance grades over the lifespan.* ***(A)*** *Predicted amygdala volume as a function of age for grade 1 individuals.* ***(B)*** *Predicted amygdala volume as a function of age for grade 2 individuals.* ***(C)*** *Predicted amygdala volume as a function of age for grade 3 individuals.* ***(D)*** *Predicted amygdala volume as a function of age for grade 4 individuals. Second row* ***(E–H)****: Predicted hippocampal volume across social tolerance grades over the lifespan.* ***(E)*** *Predicted hippocampal volume as a function of age for grade 1 individuals.* ***(F)*** *Predicted hippocampal volume as a function of age for grade 2 individuals.* ***(G)*** *Predicted hippocampal volume as a function of age for grade 3 individuals.* ***(H)*** *Predicted hippocampal volume as a function of age for grade 4 individuals.*

Discussion

We studied for the first time the neuroanatomical foundation of the naturally observed diversity of behavioral traits within the *Macaca* genus. We have assembled a unique database representing nearly half of the known macaque species, with a variety of ages, sexes, and origins. Our investigation focused on the subcortical structures of the brain and more especially the amygdala. This set of nuclei sometimes referred to as a hub of brain networks related to sociality and their social lives (Bickart et al., 2014) are well known for their roles in the stress response (Hölzel et al., 2010), emotional regulation and social cognition (Noonan et al., 2014b; Bickart et al., 2014; Amaral et al., 2003). Based on post-mortem MRI acquisitions from 12 of the 25 macaque species, we showed that amygdala volume correlated with the social tolerance grade and increased with the level of the social grade. Secondly, grade 4 species had a significantly higher amygdala volume at the start of their lives, which decreased over time, compared with grade 1 species, which showed the opposite trend. Finally, the volume of the hippocampus was constant for grade 1 and 4 species, with a higher volume for the most tolerant species. In accordance with our hypotheses (**Table 1**), our findings substantiated the assertions that (i) social tolerance is rooted in neuroanatomical differences that can be detected at an early stage of individuals' development, (ii) social styles exert differential influence on subcortical structures throughout individuals' lifespan and (iii) such phenomenon should be mainly driven by the socio-cognitive demands that vary with species social style (as evidenced by the higher volumes of amygdala and hippocampus in high tolerant species).

A neuroanatomical account for social tolerance differences

The social tolerance grades are based on previous ethological observations of behaviors across different species of the genus. From these observations, we identified three major cognitive processes—socio-cognitive demands, social predictability, and inhibitory control (see Table 1)—that underpin the observed behaviors. Among the behaviors we classified with "high social-cognitive demand", several have been previously described in the literature as particularly discriminating between grades 1 and 4. It included greater social network density in grade 4 species (a consequence of, *inter alia*, low nepotism in tolerant species, facilitating interactions between unaffiliated conspecifics) (Balasubramaniam et al., 2018; Sueur et al., 2011), more complex facial mimics as well as a more complex communication system (Dobson, 2012; Rincon et al., 2023; Scopa and Palagi, 2016; Zannella et al., 2017), a significantly higher rate of reconciliation (Thierry, 2007), and a higher frequency of cooperative behaviors, including male-to-male coalition behaviors (De Waal and Luttrell, 1989; Thierry et al., 2008) in in grade 4 species. Based on the role of the amygdala in the inhibition or activation

of impulsivity and aggression (Gopal et al., 2013), we had assumed that species of high social tolerance grade would have presented a smaller amygdala in size compared to grade 1. Given the observed inverse correlation between amygdala volume and the aforementioned behavioral traits, we postulated that additional neural mechanisms—particularly those involving cortical regions associated with social and emotional regulation—may play a critical role in underpinning the heightened aggressiveness and impulsivity observed in species with high social intolerance (Balasubramaniam et al., 2012; Loyant et al., 2023; Thierry, 2007). fMRI in humans have shown that different nuclei of the amygdala contribute to different aspect of human social life (Bickart et al., 2014). Future studies will aim at investigating the contribution of amygdala nuclei at the individual nucleus level. One could also suggest that the positive correlation with social tolerance reflects mechanisms associated with the more complex social environment of grade 4 species. Amygdala volume has been shown to correlate positively with social network complexity in grade 1 species, as measured by the social network size of individuals (Sallet et al., 2011), or by the social status of the animals (Noonan et al., 2014b).

We are then led to question the nature versus nurture origin of the social tolerance effect on amygdala volume. In light of findings from early cross-fostering experiments (De Waal and Johanowicz, 1993) and our own results, social tolerance grades can be viewed both as an innate trait—reflected in differences in amygdala size observed at a young age between grade 1 and grade 4 species—and as an acquired characteristic shaped by environmental factors. These environmental influences may stem from social interactions specific to each species' environment (Beltrán Francés et al., 2020), as well as from broader ecological contexts in which the species have evolved, evidenced by volume variations over the lifespan and changes in tolerance seen in cross-fostered individuals (De Waal and Johanowicz, 1993). It was unexpected to observe that the developmental trajectory of the amygdala in tolerant species does not align with the trajectory previously described in intolerant species, as well as in human subjects (Schumann et al., 2019; Uematsu et al., 2012). This finding raises the need to perform longitudinal studies that integrate behavioral and neuroanatomical data which could provide a clearer understanding of the relationship between social environments and brain development (Song et al., 2021). Regarding hippocampal volume, our findings indicate a consistent hippocampal volume throughout life across grade 1 and 4 species. This stability in hippocampal volume across grades warrants further exploration to clarify its role within varying social systems and cognitive demands. While these findings were beyond the primary scope of our study, they open promising avenues for future research.

This observation may be attributed to two potential factors: environmental chronic stress (due to lower social predictability) and a lower level of socio-cognitive demands. Environmental stress, as evidenced by low reconciliation rates, high dominance asymmetry, and low affiliative contact rates (Thierry, 2021, 2007, 2000), may contribute to the observed reduction in hippocampal volume. Additionally, a low level of socio-cognitive demands may also play a role. However, as previously mentioned, Tonkean macaques - a species with a high tolerance grade - are described as having a high rate of unpredictability in their social environment, inducing higher basal cortisol level, suggesting a higher level of chronic social stress (Sadoughi et al., 2021; Vandeleest et al., 2016) and, according to the literature resulting in a smaller hippocampal volume (Kim et al., 2015; Lyons et al., 2007) for these tolerant species. Yet tolerant species have a larger hippocampus than intolerant species. From these results, we can hypothesize that the unpredictability described in the literature has less subcortical neuroanatomical consequences on hippocampal size than socio-cognitive demands (Han et al., 2021). This is in line with the hypothesis that varying socio-cognitive demands may lead to changes in brain structure related to species social style.

Limits of the study and future directions

While our dataset is comprehensive in terms of the number of macaque species included certain limitations must be acknowledged. Although we explained interspecies variability, the addition of further individuals per species will help better capture the intraspecies variability in future studies. Furthermore, one will benefit from additional information about each subject. While considered in our modelling, the social living and husbandry conditions of the individuals in our dataset remain poorly documented. The living environment has been considered, and the size of social groups for certain individuals, particularly those from the CdP, has been ascertained. However, these social characteristics have not been determined for all individuals in the dataset. As previously stated, the social environment has a significant impact on the volumetry of certain regions. Furthermore, there is a dearth of data regarding the hierarchy of the subjects under study and the stress they experience in accordance with their hierarchical rank and predictability of social outcomes position (McCowan et al., 2022).

Cognitive and neural perspectives on our understanding of social tolerance

Future directions that bridge behavior, cognition, and neuroanatomy may allow to deepen our understanding of social tolerance among macaque species. From a neural perspective, studying the cortical regions associated with social tolerance represents a promising yet ambitious goal. In fact, there is an existing variability between primate species in cerebral organization (Amiez et al., 2023, 2019) which is likely to be found across the *Macaca* genus.

Considering this cerebral variability would demands extensive efforts to properly assess interspecies differences, making it beyond the scope of the current study that focus on subcortical areas. However, as a starting point, exploring the connections between the amygdala, hippocampus, and medial prefrontal cortex could provide crucial insights into the neural correlates of social tolerance. These regions are central to stress regulation, socio-cognitive processing, and decision-making, all of which are likely impacted by social tolerance grades (Caetano et al., 2021; Coplan et al., 2014; Kim et al., 2015; Phelps and LeDoux, 2005; Sapolsky et al., 1990). In humans, repeated positive or stressful experiences have been demonstrated to alter the size of ROIs such as the hippocampus or amygdala (Davidson and McEwen, 2012) and impair neuroplasticity (Phelps, 2006). Neuronal plasticity and learning have been identified as contributing factors to variations in the ROI volume, including the amygdala and hippocampus, particularly in humans (Maguire et al., 2000; Taren et al., 2013). Additionally, our conceptual framework opens avenues for advanced neuroimaging techniques such as diffusion tensor imaging (DTI) (Howard et al., 2023; Zhang et al., 2013) or multiparametric MRI (Mulholland et al., 2024), which could be used to explore white matter connectivity or microstructural changes. Our findings also emphasize the need to develop individual-level measures of social tolerance (Dubuc et al., 2012; DeTroy et al., 2021). Fine-tuning these measures would allow more precise correlations between behavioral data and neuroanatomical features. By operationalizing the concept of social tolerance on cognitive dimensions, our work aims at enriching the framework through which primate sociality is currently studied.

Conclusion

Our study provides groundbreaking insights into the relationship between amygdala volume and social tolerance in macaques, offering an innovative perspective on the neuroanatomical basis of social cognition. Using a comparative approach across 12 macaque species, we uncovered a revealing relationship: low-tolerance species start their life with a smaller amygdala compared to their socially tolerant counterparts. In addition, intolerant species show an increase in amygdala volume, whereas highly tolerant species show the opposite trend. These findings challenge conventional expectations of the amygdala's primary involvement in emotional processes and highlight the complexity of the amygdala's role in social cognition.

The observed differences in amygdala volume with respect to social tolerance grades suggest that the development and plasticity of the amygdala seem to be intricately linked to the social environment and experiences of the species. Larger amygdala in socially tolerant species may reflect an enhanced capacity to process complex social information, facilitating better social

interactions, cooperative behavior, and conflict management. Alternatively, the observed increase in amygdala volume in socially intolerant species over time may be explained by heightened socio-cognitive demands, rather than being solely attributed to chronic stress or emotional reactivity. While earlier studies emphasized the role of the amygdala in stress response, recent findings are in lines with our results which suggest that amygdala's functions extend to broader aspects of social cognition. These findings have profound implications for our understanding of social brain evolution as well as underscoring the importance of developmental stage and the social environment being crucial drivers of neuroanatomical adaptations. This study, at the interface of primatology and cognitive neuroscience, also provides a framework for investigating the impact of the social environment on brain development and pave the way for future research to unravel the complexities of brain evolution and sociality.

Material & Methods

Brain specimen collection

To allow comprehensive cross-species comparisons in the *Macaca* genus, a dataset of 42 *post-mortem* specimens has been constituted through collaborations with multiple research centers, each contributing unique expertise and resources (**Table 2**). The collaborating institutions included **(Table S1)**:

The Centre de Primatologie de l'Université de Strasbourg (CdP): provided valuable brain data derived from 20 brain samples. One sample (*M. nigra*) was acquired in the frame of a local collaboration with the zoo of Mulhouse (https://www.zoo-mulhouse.com/).

Samples from INDI-PRIME-DE (Milham et al., 2018): The Japan Monkey Center provided 5 *post-mortem* MRI acquisitions to the dataset (Sakai et al., 2018). Utrecht University: contributed to the dataset with 13 *post-mortem* MRI acquisitions (Navarrete et al., 2018).

INSERM-Oxford University: 5 *post-mortem* MRI acquisitions came from this collaboration. This addition offered more variety of acquired data mostly in age and sex (Milham et al., 2018).

Ethical considerations

The study was conducted in accordance with ethical guidelines and was approved by the ethical committee of the Centre de Primatologie de l'Université de Strasbourg which is authorized to house NHP (registration B6732636). The research further complied with the EU Directive 2010/63/EU for animal experiments. All subjects from the CdP died of natural or accidental cause; no macaque was euthanized in the sole frame of the project. These specimens originated from CdP, and their collection followed rigorous ethical considerations. The specimens were either obtained from previous collections—where full bodies were preserved in dedicated freezers—or from individuals of the CdP that had died from natural causes. The post-mortem MRI data from INSERM- Oxford University were acquired from deceased animals that died of causes unrelated to the present research project. As such, the research did not require a Home Office License as defined by the Animals (Scientific Procedures) Act 1986 of the United Kingdom.

Brain extraction technique

Post-mortem MRI images acquisition of macaque brains is central to our study, more specifically, in translational studies of homologous brain regions. Brain extraction is a crucial process in neuroscience research for studying the internal brain structure of animals. Through the acquisition at the CdP of 20 *post-mortem* anatomical MRI scans of brains from six different species of macaques, we were able to refine a brain extraction technique - whether previously

frozen or fresh - to minimize specimen handling artefacts and obtain image quality suitable for optimal use by the scientific community. The detailed extraction technique protocol established and used for our brain extractions is available in **Document S1**. Briefly, the head is reclined forward to expose the neck, muscles are removed to access the atlanto-occipital junction, which is then incised to allow head dislocation (**Figure S1**). An osteotome and hammer are used, ensuring no cerebellar herniation. The skull cap is carefully drilled using a rotary tool and removed (see **Figure S1. A, B** and **Table S2** for required tools), and the brain is extracted by severing the olfactory peduncles, internal carotid arteries, and cranial nerves. Specimens are then fixed in 10% buffered formaldehyde for 7 days (see **Figure S1. D.**) and in phosphate buffered saline (PBS) for 3-4 days before being placed in Fluorinert™ for MRI acquisition, ensuring minimal air bubbles and optimal image quality (Sébille et al., 2019) see **Figure S2**).

Sampling methods & measurements

Structural images were collected through both the open access databases and collaborations (Milham et al., 2018; Navarrete et al., 2018; Sakai et al., 2018), but also carried out at the IRIS platform of the ICube laboratory in Strasbourg for *post-mortem* samples kept at the CdP (see **Table S3** for the information relating to the acquisition of anatomical MRI images). The final dataset consists of 42 anatomical scans after pruning data with missing age or sex information (10 individuals), with both T_1 and T_2-weighted images. Due to their different origins, the images in the dataset did not follow the exact same acquisition protocols (different scanners and acquisition parameters, **Table 2**). In addition, *post-mortem* brain preservation and perfusion protocols are different, which may also influence the images obtained. Volume measurements were performed using a semi-automatic method to register individual images to the Subcortical Atlas of the Rhesus Macaque (SARM) (Hartig et al., 2021) **(Figure S1.E.)**. Due the large orientation discrepancies across the research centers, the images were first manually realigned (translation and rotation) with the atlas using ITK-SNAP (Yushkevich et al., 2006), then non-linearly registered using ANTs (Avants et al., 2011). The segmentation maps of the atlas were then transported to the subject space to extract the volume of the regions of interest. **Figure S1** details the image processing for volume extractions (see **Figure S2**). To ensure the accuracy of the SARM on our dataset, which includes 11 species other than *M. mulatta* (the species used for SARM development (Hartig et al., 2021)), we calculated the Dice Similarity Coefficient (DSC) (Zou et al., 2004). This was done by manually segmenting, using a tablet (Wacom Cintiq® 16 and ITK SNAP software), the amygdala in each acquisition and comparing the overlapping voxels between the manual segmentation and the SARM

segmentation. With a DSC of 0.96, we confirm the robust performance of the SARM across our entire dataset.

Final dataset characteristics

The dataset is composed of 12 distinct macaque species with a total of 42 individual specimens for analysis. There is a strong sex imbalance with more females than males. The age range spans from 1 to 44.20 years, with an average age of 18.2 ± 9.4 years (standard deviation) (**Figure 1. B, D**.) with two outliers above 35 years old. Most importantly, based on our research question, the social grade distribution of our dataset (**Figure 1. A**.) is more represented by grade 1 than grade 4 species as these species are very rare in zoo or in research centers and most of them protected as endangered species. The MRI acquisitions from the 42 individuals were standardized to the NMT template(Jung et al., 2021). Data included amygdala or hippocampus volume and a computed brain "total volume" which only excludes the myelencephalon and the cerebellum for reliability. In fact, the integrity of these subcortical structures heavily depends on the quality and technics used for brain extraction methods.

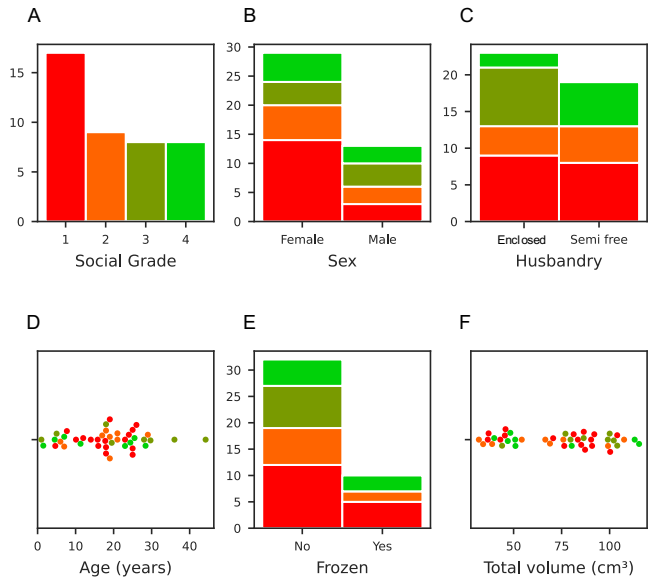

***Figure 1**: **Dataset characteristics relative to the social grade.** In red: social tolerance grade 1, orange: grade 2, olive: grade 3, and green: grade 4. **(A)** Social tolerance grade distribution, where grade 1 is overrepresented due to the prevalence of Macaca mulatta in laboratories. **(B)** Sex distribution: There was a significant imbalance in the sample, with females outnumbering males (2:1 ratio). **(C)** Husbandry distribution of the individuals (enclosed and semi-free ranging conditions) **(D)** Age distribution: The cohort had a relatively even age distribution with a notable peak in the 20s. **(E)** The frozen status distribution. **(F)** Total brain volume distribution, excluding the myelencephalon and cerebellum due to variation in their preservation.*

Modelling approach

To investigate the subcortical correlates of social tolerance in macaques, we used a multivariate Bayesian linear model with normal likelihood, the observed data being the amygdala and hippocampus volume. The predictors in our model were the intercept, social grade, age, sex, husbandry, whether the brain had been previously frozen, total volume, the interaction between social grade and age, and the covariance between the observations. We used wide priors, whose locations and scales were derived from the data. We assessed the quality of the model by comparing the predicted data to the observed data, and by checking the R^2 of the model. New data was predicted to study the interaction and the age-social grade trajectory, and the difference in volume between social grades. The predictions were made using the model on all social grades, on females aged from 1 to 40, with a total volume of 85 cm^3.

Acknowledgement

The authors are grateful to the University of Strasbourg, the CNRS and Silabe (https://silabe.com/) for supporting this research and providing expert animal care. This work was further funded by ANR-21-CE37-0016 to S.B and J. S. This work is co funded by the French State Region contract CPER I2MT (2014-2021), R-IRM (2021-2027) and by the European Union through the European Regional Development Fund “FEDER Grand Est”. This work was performed on IRIS platform of ICube lab, member of France Life Imaging network (grant ANR 11 INBS 0006). We extend our gratitude to the PRIME-DE open science initiative, particularly the Utrecht database, as well as the Japan Monkey Center for providing access to their open science resources. Additionally, we sincerely thank Aurore de Cauwer (from ICube) for her invaluable assistance at the early stages in the MRI data acquisition. The Wellcome Centre for Integrative Neuroimaging is supported by core funding from the Wellcome Trust (203139/Z/16/Z).

Author’s contribution

S.B. and S.S. conceptualized the research; C.P., S.B., J.S. and S.S. developed the methodology, S.S. performed the data curation, J.L. performed the formal analysis, S.S., S.B. C.P., J.S. and M.L. performed the investigation; S.S., J.L. and S.B. wrote the original manuscript; S.B. and J.S. acquired the funding. All the authors reviewed the manuscript.

Declaration of interests

The authors declare no competing interests.

Data availability

The data associated with this study are available at DOI : 10.17605/OSF.IO/AQMSW) or at this link https://doi.org/10.17605/OSF.IO/AQMSW .

Supplemental information

Table S1: Species and data collection centers in the dataset.

Document S1: Detailed brain extraction procedure. Table S2, Figures S1-S2.

Table S3: Information relating to the acquisition of anatomical MRI images and the procedures for fixing and preserving post-mortem samples according to the different institutes.

References

Amaral DG, Bauman MD, Capitanio JP, Lavenex P, Mason WA, Mauldin-Jourdain ML, Mendoza SP. 2003. The amygdala: is it an essential component of the neural network for social cognition? *Neuropsychologia* **41**:517–522. doi:10.1016/S0028-3932(02)00310-X

Amiez C, Sallet J, Giacometti C, Verstraete C, Gandaux C, Morel-Latour V, Meguerditchian A, Hadj-Bouziane F, Ben Hamed S, Hopkins WD, Procyk E, Wilson CRE, Petrides M. 2023. A revised perspective on the evolution of the lateral frontal cortex in primates. *Sci Adv* **9**:eadf9445. doi:10.1126/sciadv.adf9445

Amiez C, Sallet J, Hopkins WD, Meguerditchian A, Hadj-Bouziane F, Ben Hamed S, Wilson CRE, Procyk E, Petrides M. 2019. Sulcal organization in the medial frontal cortex provides insights into primate brain evolution. *Nat Commun* **10**:3437. doi:10.1038/s41467-019-11347-x

Avants BB, Tustison NJ, Song G, Cook PA, Klein A, Gee JC. 2011. A Reproducible Evaluation of ANTs Similarity Metric Performance in Brain Image Registration. *Neuroimage* **54**:2033–2044. doi:10.1016/j.neuroimage.2010.09.025

Balasubramaniam KN, Beisner BA, Berman CM, De Marco A, Duboscq J, Koirala S, Majolo B, MacIntosh AJ, McFarland R, Molesti S, Ogawa H, Petit O, Schino G, Sosa S, Sueur C, Thierry B, de Waal FBM, McCowan B. 2018. The influence of phylogeny, social style, and sociodemographic factors on macaque social network structure. *Am J Primatol* **80**:e22727. doi:10.1002/ajp.22727

Balasubramaniam KN, Dittmar K, Berman CM, Butovskaya M, Cooper MA, Majolo B, Ogawa H, Schino G, Thierry B, De Waal FBM. 2012. Hierarchical Steepness, Counter-Aggression, and Macaque Social Style Scale. *American Journal of Primatology* **74**:915–925. doi:10.1002/ajp.22044

Beltrán Francés V, Castellano-Navarro A, Illa Maulany R, Ngakan PO, MacIntosh AJJ, Llorente M, Amici F. 2020. Play behavior in immature moor macaques (Macaca maura) and Japanese macaques (Macaca fuscata). *American Journal of Primatology* **82**:e23192. doi:10.1002/ajp.23192

Berman C, Thierry B. 2010. Variation in kin bias: species differences and time constraints in macaques. doi:10.1163/000579510X539691

Bickart KC, Dickerson BC, Feldman Barrett L. 2014. The amygdala as a hub in brain networks that support social life. *Neuropsychologia* **63**:235–248. doi:10.1016/j.neuropsychologia.2014.08.013

Bickart KC, Wright CI, Dautoff RJ, Dickerson BC, Barrett LF. 2011. Amygdala volume and social network size in humans. *Nat Neurosci* **14**:163–164. doi:10.1038/nn.2724

527 Caetano I, Amorim L, Soares JM, Ferreira S, Coelho A, Reis J, Santos NC, Moreira PS,
528 Marques P, Magalhães R, Esteves M, Picó-Pérez M, Sousa N. 2021. Amygdala size
529 varies with stress perception. *Neurobiol Stress* **14**:100334.
530 doi:10.1016/j.ynstr.2021.100334
531 Carlo CN, Stefanacci L, Semendeferi K, Stevens CF. 2010. Comparative analyses of the
532 neuron numbers and volumes of the amygdaloid complex in old and new world primates.
533 *Journal of Comparative Neurology* **518**:1176–1198.
534 doi:https://doi.org/10.1002/cne.22264
535 Cooper EB, Brent LJ, Snyder-Mackler N, Singh M, Sengupta A, Khatiwada S, Malaivijitnond
536 S, Qi Hai Z, Higham JP. 2022. The rhesus macaque as a success story of the
537 Anthropocene. *eLife* **11**:e78169. doi:10.7554/eLife.78169
538 Coplan JD, Fathy HM, Jackowski AP, Tang CY, Perera TD, Mathew SJ, Martinez J, Abdallah
539 CG, Dwork AJ, Pantol G, Carpenter D, Gorman JM, Nemeroff CB, Owens MJ, Kaffman
540 A, Kaufman J. 2014. Early life stress and macaque amygdala hypertrophy: preliminary
541 evidence for a role for the serotonin transporter gene. *Front Behav Neurosci* **8**.
542 doi:https://doi.org/10.3389/fnbeh.2014.00342
543 Cords M. 2012. The Behavior, Ecology, and Social Evolution of Cercopithecine Monkeys In:
544 Mitani JC, Call J, Kappeler PM, Palombit RA, Silk JB, editors. The Evolution of Primate
545 Societies. University of Chicago Press. pp. 91–112.
546 Dark HE, Harnett NG, Knight AJ, Knight DC. 2021. Hippocampal volume varies with acute
547 posttraumatic stress symptoms following medical trauma. *Behav Neurosci* **135**:71–78.
548 doi:10.1037/bne0000419
549 Davidson RJ, McEwen BS. 2012. Social influences on neuroplasticity: Stress and
550 interventions to promote well-being. *Nat Neurosci* **15**:689–695. doi:10.1038/nn.3093
551 De Waal FB, Johanowicz DL. 1993. Modification of Reconciliation Behavior Through Social
552 Experience: An Experiment with Two Macaque Species. *Child Development* **64**:897–
553 908. doi:10.2307/1131225
554 De Waal FB, Luttrell LM. 1985. The formal hierarchy of rhesus macaques: An investigation of
555 the bared-teeth display. *American Journal of Primatology* **9**:73–85.
556 doi:10.1002/ajp.1350090202
557 De Waal FBM, Luttrell LM. 1989. Toward a comparative socioecology of the genus Macaca:
558 Different dominance styles in rhesus and stumptail monkeys. *Am J Primatol* **19**:83–109.
559 doi:10.1002/ajp.1350190203
560 DeTroy SE, Haun DBM, van Leeuwen EJC. 2021. What isn't social tolerance? The past,
561 present, and possible future of an overused term in the field of primatology. *Evolutionary*
562 *anthropology*. doi:10.1002/evan.21923
563 Dobson SD. 2012. Coevolution of Facial Expression and Social Tolerance in Macaques.

American Journal of Primatology **74**:229–235. doi:10.1002/ajp.21991

Duboscq J, Agil M, Engelhardt A, Thierry B. 2014. The function of postconflict interactions: new prospects from the study of a tolerant species of primate. *Animal Behaviour* **87**:107–120. doi:10.1016/j.anbehav.2013.10.018

Duboscq J, Micheletta J, Agil M, Hodges K, Thierry B, Engelhardt A. 2013. Social Tolerance in Wild Female Crested Macaques (Macaca nigra) in Tangkoko-Batuangus Nature Reserve, Sulawesi, Indonesia. *Am J Primatol* **75**:361–375. doi:10.1002/ajp.22114

Dubuc C, Hughes KD, Cascio J, Santos LR. 2012. Social tolerance in a despotic primate: co-feeding between consortship partners in rhesus macaques. *Am J Phys Anthropol* **148**:73–80. doi:10.1002/ajpa.22043

Dunbar RIM. 2009. The social brain hypothesis and its implications for social evolution. *Ann Hum Biol* **36**:562–572. doi:10.1080/03014460902960289

Ghosh A, Thakur M, Singh SK, Dutta R, Sharma LK, Chandra K, Banerjee D. 2022. The Sela macaque (*Macaca selai*) is a distinct phylogenetic species that evolved from the Arunachal macaque following allopatric speciation. *Molecular Phylogenetics and Evolution* **174**:107513. doi:10.1016/j.ympev.2022.107513

Gopal A, Clark E, Allgair A, D'Amato C, Furman M, Gansler DA, Fulwiler C. 2013. Dorsal/ventral parcellation of the amygdala: Relevance to impulsivity and aggression. *Psychiatry Research: Neuroimaging* **211**:24–30. doi:10.1016/j.pscychresns.2012.10.010

Haley GE, McGuire A, Berteau-Pavy D, Weiss A, Patel R, Messaoudi I, Urbanski HF, Raber J. 2012. Measures of anxiety, amygdala volumes, and hippocampal scopolamine phMRI response in elderly female rhesus macaques. *Neuropharmacology* **62**:385–390. doi:10.1016/j.neuropharm.2011.08.014

Han M, Jiang G, Luo H, Shao Y. 2021. Neurobiological Bases of Social Networks. *Front Psychol* **12**. doi:10.3389/fpsyg.2021.626337

Hartig R, Glen D, Jung B, Logothetis NK, Paxinos G, Garza-Villarreal EA, Messinger A, Evrard HC. 2021. The Subcortical Atlas of the Rhesus Macaque (SARM) for neuroimaging. *NeuroImage* **235**:117996. doi:10.1016/j.neuroimage.2021.117996

Heldstab SA, Isler K, Graber SM, Schuppli C, van Schaik CP. 2022. The economics of brain size evolution in vertebrates. *Curr Biol* **32**:R697–R708. doi:10.1016/j.cub.2022.04.096

Hölzel BK, Carmody J, Evans KC, Hoge EA, Dusek JA, Morgan L, Pitman RK, Lazar SW. 2010. Stress reduction correlates with structural changes in the amygdala. *Social Cognitive and Affective Neuroscience* **5**:11–17. doi:10.1093/scan/nsp034

Howard AFD, Huszar IN, Smart A, Cottaar M, Daubney G, Hanayik T, Khrapitchev AA, Mars RB, Mollink J, Scott C, Sibson NR, Sallet J, Jbabdi S, Miller KL. 2023. An open resource combining multi-contrast MRI and microscopy in the macaque brain. *Nat Commun*

14:4320. doi:10.1038/s41467-023-39916-1

Howell BR, Grand AP, McCormack KM, Shi Y, LaPrarie J, Maestripieri D, Styner MA, Sanchez MM. 2014. Early Adverse Experience Increases Emotional Reactivity in Juvenile Rhesus Macaques: Relation to Amygdala Volume. *Dev Psychobiol* **56**:1735–1746. doi:10.1002/dev.21237

Isa T, Yamane I, Hamai M, Inagaki H. 2009. Japanese macaques as laboratory animals. *Exp Anim* **58**:451–457. doi:10.1538/expanim.58.451

Joly M, Micheletta J, De Marco A, Langermans JA, Sterck EHM, Waller BM. 2017. Comparing physical and social cognitive skills in macaque species with different degrees of social tolerance. *Proc Royal Soc B* **284**:20162738. doi:10.1098/rspb.2016.2738

Jung B, Taylor PA, Seidlitz J, Sponheim C, Perkins P, Ungerleider LG, Glen D, Messinger A. 2021. A comprehensive macaque fMRI pipeline and hierarchical atlas. *NeuroImage* **235**:117997. doi:10.1016/j.neuroimage.2021.117997

Kanai R, Bahrami B, Roylance R, Rees G. 2012. Online social network size is reflected in human brain structure. *Proc Royal Soc B* **279**:1327–1334. doi:10.1098/rspb.2011.1959

Kim EJ, Pellman B, Kim JJ. 2015. Stress effects on the hippocampus: a critical review. *Learn Mem* **22**:411–416. doi:10.1101/lm.037291.114

Loyant L, Waller BM, Micheletta J, Meunier H, Ballesta S, Joly M. 2023. Tolerant macaque species are less impulsive and reactive. *Anim Cogn* **26**:1453–1466. doi:25

Lyons DM, Parker KJ, Zeitzer JM, Buckmaster CL, Schatzberg AF. 2007. Preliminary evidence that hippocampal volumes in monkeys predict stress levels of adrenocorticotropic hormone. *Biol Psychiatry* **62**:1171–1174. doi:10.1016/j.biopsych.2007.03.012

Lyons DM, Yang C, Sawyer-Glover AM, Moseley ME, Schatzberg AF. 2001. Early life stress and inherited variation in monkey hippocampal volumes. *Arch Gen Psychiatry* **58**:1145–1151. doi:10.1001/archpsyc.58.12.1145

Maguire EA, Gadian DG, Johnsrude IS, Good CD, Ashburner J, Frackowiak RS, Frith CD. 2000. Navigation-related structural change in the hippocampi of taxi drivers. *Proc Natl Acad Sci U S A* **97**:4398–4403. doi:10.1073/pnas.070039597

ManyPrimates, Aguenounon G, Allritz M, Altschul D, Ballesta S, Beaud A, Bohn M, Bornbusch S, Brandão A, Brooks J, Bugnyar T, Burkart J, Bustamante L, Call J, Canteloup C, Cao C, Caspar K, da Silva D, de Sousa A, DeTroy S, Duguid S, Eppley T, Fichtel C, Fischer J, Gong C, Grange J, Grebe N, Hanus D, Haun D, Haux L, Héjja-Brichard Y, Helman A, Hernadi I, Hernandez-Aguilar RA, Herrmann E, Hopper L, Howard L, Huang L, Huskisson S, Jacobs I, Jin Z, Joly M, Kano F, Keupp S, Kiefer E, Knakker B, Kóczán K, Kraus L, Kwok SC, Lefrançois M, Lewis L, Liu S, Llorente M, Lonsdorf E, Loyant L, Majecka K, Maurits L, Meunier H, Mobili F, Morino L, Motes-Rodrigo A, Nijman V, Ihomi C, Persson T, Pietraszewski D, Reátiga Parrish J, Roig A, Sánchez-Amaro A, Sato Y,

638 Sauciuc G-A, Schrock A, Schweinfurth M, Seed A, Shearer C, Šlipogor V, Su Y,
639 Sutherland K, Tan J, Taylor D, Troisi C, Völter C, Warren E, Watzek J, Zablocki-Thomas
640 P. 2022. The Evolution of Primate Short-Term Memory. *AB&C* **9**:428–516.
641 doi:10.26451/abc.09.04.06.2022
642 Maranesi M, Livi A, Fogassi L, Rizzolatti G, Bonini L. 2014. Mirror neuron activation prior to
643 action observation in a predictable context. *J Neurosci* **34**:14827–14832.
644 doi:10.1523/JNEUROSCI.2705-14.2014
645 McCowan B, Vandeleest J, Balasubramaniam K, Hsieh F, Nathman A, Beisner B. 2022.
646 Measuring dominance certainty and assessing its impact on individual and societal
647 health in a nonhuman primate model: a network approach. *Philosophical Transactions*
648 *of the Royal Society B: Biological Sciences* **377**:20200438. doi:10.1098/rstb.2020.0438
649 Meguerditchian A, Marie D, Margiotoudi K, Roth M, Nazarian B, Anton J-L, Claidière N. 2021.
650 Baboons (Papio anubis) living in larger social groups have bigger brains. *Evolution and*
651 *Human Behavior* **42**:30–34. doi:10.1016/j.evolhumbehav.2020.06.010
652 Meyer JS, Hamel AF. 2014. Models of Stress in Nonhuman Primates and Their Relevance for
653 Human Psychopathology and Endocrine Dysfunction. *ILAR Journal* **55**:347–360.
654 doi:10.1093/ilar/ilu023
655 Milham MP, Ai L, Koo B, Xu T, Amiez C, Balezeau F, Baxter MG, Blezer ELA, Brochier T,
656 Chen A, Croxson PL, Damatac CG, Dehaene S, Everling S, Fair DA, Fleysher L,
657 Freiwald W, Froudist-Walsh S, Griffiths TD, Guedj C, Hadj-Bouziane F, Ben Hamed S,
658 Harel N, Hiba B, Jarraya B, Jung B, Kastner S, Klink PC, Kwok SC, Laland KN, Leopold
659 DA, Lindenfors P, Mars RB, Menon RS, Messinger A, Meunier M, Mok K, Morrison JH,
660 Nacef J, Nagy J, Rios MO, Petkov CI, Pinsk M, Poirier C, Procyk E, Rajimehr R, Reader
661 SM, Roelfsema PR, Rudko DA, Rushworth MFS, Russ BE, Sallet J, Schmid MC,
662 Schwiedrzik CM, Seidlitz J, Sein J, Shmuel A, Sullivan EL, Ungerleider L, Thiele A,
663 Todorov OS, Tsao D, Wang Z, Wilson CRE, Yacoub E, Ye FQ, Zarco W, Zhou Y,
664 Margulies DS, Schroeder CE. 2018. An Open Resource for Non-human Primate
665 Imaging. *Neuron* **100**:61-74.e2. doi:10.1016/j.neuron.2018.08.039
666 Mulholland MM, Hecht E, Wesley MJ, Hopkins WD. 2024. Long term impacts of early social
667 environment on chimpanzee white matter. *Sci Rep* **14**:29879. doi:10.1038/s41598-024-
668 81238-9
669 Navarrete AF, Blezer ELA, Pagnotta M, de Viet ESM, Todorov O, Lindenfors P, Laland K,
670 Reader SM. 2018. Primate Brain Anatomy: New Volumetric MRI Measurements for
671 Neuroanatomical Studies. *Brain Behav Evol* **91**:1–9. doi:10.1159/000488136
672 Noonan MP, Sallet J, Mars RB, Neubert FX, O'Reilly JX, Andersson JL, Mitchell AS, Bell AH,
673 Miller KL, Rushworth MFS. 2014a. A Neural Circuit Covarying with Social Hierarchy in
674 Macaques. *PLoS Biology* **12**:e1001940. doi:10.1371/journal.pbio.1001940

Noonan MP, Sallet J, Mars RB, Neubert FX, O'Reilly JX, Andersson JL, Mitchell AS, Bell AH, Miller KL, Rushworth MFS. 2014b. A Neural Circuit Covarying with Social Hierarchy in Macaques. *PLOS Biol* **12**:e1001940. doi:10.1371/journal.pbio.1001940

Parkinson C, Kleinbaum AM, Wheatley T. 2017. Spontaneous neural encoding of social network position. *Nat Hum Behav* **1**:1–7. doi:10.1038/s41562-017-0072

Perelman P, Johnson WE, Roos C, Seuánez HN, Horvath JE, Moreira MAM, Kessing B, Pontius J, Roelke M, Rumpler Y, Schneider MPC, Silva A, O'Brien SJ, Pecon-Slattery J. 2011. A Molecular Phylogeny of Living Primates. *PLoS Genet* **7**:e1001342. doi:10.1371/journal.pgen.1001342

Phelps EA. 2006. Emotion and cognition: insights from studies of the human amygdala. *Annu Rev Psychol* **57**:27–53. doi:10.1146/annurev.psych.56.091103.070234

Phelps EA, LeDoux JE. 2005. Contributions of the amygdala to emotion processing: from animal models to human behavior. *Neuron* **48**:175–187. doi:10.1016/j.neuron.2005.09.025

Rebout N, De Marco A, Lone J-C, Sanna A, Cozzolino R, Micheletta J, Sterck EHM, Langermans JAM, Lemasson A, Thierry B. 2020. Tolerant and intolerant macaques show different levels of structural complexity in their vocal communication. *Proceedings of the Royal Society B: Biological Sciences* **287**:20200439. doi:10.1098/rspb.2020.0439

Rebout N, De Marco A, Sanna A, Micheletta J, Lone J-C, van den Berg RF, Sterck EHM, Langermans JAM, Thierry B, Lemasson A. 2022. Tolerant and intolerant macaques differ in the context specificity of their calls and how they 'comment' on the interactions of others. *Behav Ecol Sociobiol* **76**:67. doi:10.1007/s00265-022-03177-7

Rincon AV, Waller BM, Duboscq J, Mielke A, Pérez C, Clark PR, Micheletta J. 2023. Higher social tolerance is associated with more complex facial behavior in macaques. *Elife* **12**:RP87008. doi:10.7554/eLife.87008

Sadoughi B, Lacroix L, Berbesque C, Meunier H, Lehmann J. 2021. Effects of social tolerance on stress: hair cortisol concentrations in the tolerant Tonkean macaques (Macaca tonkeana) and the despotic long-tailed macaques (Macaca fascicularis). *Stress* **24**:1033–1041. doi:10.1080/10253890.2021.1998443

Sakai T, Hata J, Ohta H, Shintaku Y, Kimura N, Ogawa Y, Sogabe K, Mori S, Okano HJ, Hamada Y, Shibata S, Okano H, Oishi K. 2018. The Japan Monkey Centre Primates Brain Imaging Repository for comparative neuroscience: an archive of digital records including records for endangered species. *Primates* **59**:553–570. doi:10.1007/s10329-018-0694-3

Sakai T, Hata J, Shintaku Y, Ohta H, Sogabe K, Mori S, Miyabe-Nishiwaki T, Okano HJ, Hamada Y, Hirabayashi T, Minamimoto T, Sadato N, Okano H, Oishi K. 2023. The Japan Monkey Centre Primates Brain Imaging Repository of high-resolution postmortem

magnetic resonance imaging: The second phase of the archive of digital records. *NeuroImage* **273**:120096. doi:10.1016/j.neuroimage.2023.120096

Sallet J, Mars RB, Noonan MP, Andersson JL, O'Reilly JX, Jbabdi S, Croxson PL, Jenkinson M, Miller KL, Rushworth MFS. 2011. Social Network Size Affects Neural Circuits in Macaques. *Science* **334**:697–700. doi:10.1126/science.1210027

Sapolsky RM, Uno H, Rebert CS, Finch CE. 1990. Hippocampal damage associated with prolonged glucocorticoid exposure in primates. *J Neurosci* **10**:2897–2902. doi:10.1523/JNEUROSCI.10-09-02897.1990

Schumann CM, Scott JA, Lee A, Bauman MD, Amaral DG. 2019. Amygdala growth from youth to adulthood in the macaque monkey. *J Comp Neurol* **527**:3034–3045. doi:10.1002/cne.24728

Scopa C, Palagi E. 2016. Mimic me while playing! Social tolerance and rapid facial mimicry in macaques (Macaca tonkeana and Macaca fuscata). *J Comp Psychol* **130**:153–161. doi:10.1037/com0000028

Sébille SB, Rolland A-S, Welter M-L, Bardinet E, Santin MD. 2019. Post mortem high resolution diffusion MRI for large specimen imaging at 11.7 T with 3D segmented echo-planar imaging. *Journal of Neuroscience Methods* **311**:222–234. doi:10.1016/j.jneumeth.2018.10.010

Song X, García-Saldivar P, Kindred N, Wang Y, Merchant H, Meguerditchian A, Yang Y, Stein EA, Bradberry CW, Ben Hamed S, Jedema HP, Poirier C. 2021. Strengths and challenges of longitudinal non-human primate neuroimaging. *Neuroimage* **236**:118009. doi:10.1016/j.neuroimage.2021.118009

Sueur C, Petit O, De Marco A, Jacobs AT, Watanabe K, Thierry B. 2011. A comparative network analysis of social style in macaques. *Animal Behaviour* **82**:845–852. doi:10.1016/j.anbehav.2011.07.020

Taren AA, Creswell JD, Gianaros PJ. 2013. Dispositional Mindfulness Co-Varies with Smaller Amygdala and Caudate Volumes in Community Adults. *PLoS One* **8**:e64574. doi:10.1371/journal.pone.0064574

Testard C, Brent LJN, Andersson J, Chiou KL, Negron-Del Valle JE, DeCasien AR, Acevedo-Ithier A, Stock MK, Antón SC, Gonzalez O, Walker CS, Foxley S, Compo NR, Bauman S, Ruiz-Lambides AV, Martinez MI, Skene JHP, Horvath JE, Unit CBR, Higham JP, Miller KL, Snyder-Mackler N, Montague MJ, Platt ML, Sallet J. 2022. Social connections predict brain structure in a multidimensional free-ranging primate society. *Sci Adv* **8**:eabl5794. doi:10.1126/sciadv.abl5794

Thierry B. 2021. Where do we stand with the covariation framework in primate societies? *Am J Biol Anthropol* **178**. doi:10.1002/ajpa.24441

Thierry B. 2017. Macaque (Macaca)The International Encyclopedia of Primatology. John

Wiley & Sons, Ltd. pp. 1–4. doi:10.1002/9781119179313.wbprim0040

Thierry B. 2007. Unity in diversity: Lessons from macaque societies. *Evol Anthropol* **16**:224–238. doi:10.1002/evan.20147

Thierry B. 2000. Covariation of Conflict Management Patterns across Macaque SpeciesNatural Conflict Resolution. Berkeley, CA, US: University of California Press. pp. 106–128.

Thierry B, Aureli F, Nunn CL, Petit O, Abegg C, de Waal FBM. 2008. A comparative study of conflict resolution in macaques: insights into the nature of trait covariation. *Animal Behaviour* **75**:847–860. doi:10.1016/j.anbehav.2007.07.006

Thierry B, Iwaniuk AN, Pellis SM. 2000. The Influence of Phylogeny on the Social Behaviour of Macaques (Primates: Cercopithecidae, genus Macaca). *Ethology* **106**:713–728. doi:10.1046/j.1439-0310.2000.00583.x

Thierry B, Singh M, Kaumanns W. 2004. Macaque Societies: A Model for the Study of Social Organization. Cambridge University Press.

Todorov OS, Weisbecker V, Gilissen E, Zilles K, de Sousa AA. 2019. Primate hippocampus size and organization are predicted by sociality but not diet. *Proceedings of the Royal Society B: Biological Sciences* **286**:20191712. doi:10.1098/rspb.2019.1712

Tottenham N, Sheridan MA. 2010. A review of adversity, the amygdala and the hippocampus: a consideration of developmental timing. *Front Hum Neurosci* **3**. doi:10.3389/neuro.09.068.2009

Uematsu A, Matsui M, Tanaka C, Takahashi T, Noguchi K, Suzuki M, Nishijo H. 2012. Developmental Trajectories of Amygdala and Hippocampus from Infancy to Early Adulthood in Healthy Individuals. *PLoS One* **7**:e46970. doi:10.1371/journal.pone.0046970

Vandeleest JJ, Beisner BA, Hannibal DL, Nathman AC, Capitanio JP, Hsieh F, Atwill ER, McCowan B. 2016. Decoupling social status and status certainty effects on health in macaques: a network approach. *PeerJ* **4**:e2394. doi:10.7717/peerj.2394

Yushkevich PA, Piven J, Hazlett HC, Smith RG, Ho S, Gee JC, Gerig G. 2006. User-guided 3D active contour segmentation of anatomical structures: Significantly improved efficiency and reliability. *NeuroImage* **31**:1116–1128. doi:10.1016/j.neuroimage.2006.01.015

Zannella A, Stanyon R, Palagi E. 2017. Yawning and social styles: Different functions in tolerant and despotic macaques (Macaca tonkeana and Macaca fuscata). *Journal of Comparative Psychology* **131**:179–188. doi:10.1037/com0000062

Zhang D, Guo L, Zhu D, Li K, Li L, Chen H, Zhao Q, Hu X, Liu T. 2013. Diffusion Tensor Imaging Reveals Evolution of Primate Brain Architectures. *Brain Struct Funct* **218**:10.1007/s00429-012-0468–4. doi:10.1007/s00429-012-0468-4

Zou KH, Warfield SK, Bharatha A, Tempany CMC, Kaus MR, Haker SJ, Wells WM, Jolesz FA, Kikinis R. 2004. Statistical Validation of Image Segmentation Quality Based on a Spatial Overlap Index. *Acad Radiol* **11**:178–189. doi:10.1016/S1076-6332(03)00671-8

Supplementary

Table S1: Species and data collection centers in the dataset

	CdP	Utrecht University	Inserm Oxford University	Japan Monkey Center	Total
M. arctoides [3]		3			3
M. fascicularis [2]	3	1	1	1	6
M. fuscata [1]		2		2	4
M. mulatta [1]	8	1	4		13
M. nemestrina [2]	1	1			2
M. nigra [4]	1	1			2
M. silenus [3]		1			1
M. sinica [3]				1	1
M. sylvanus [3]		2			2
M. thibetana [2]	1				1
M. tonkeana [4]	6				6
M. radiata [3]				1	1
Total	20	12	5	5	42

Summary table of our dataset detailing the macaque species, the social grades [x] and the centers they originate from.

The dataset includes brain imaging data from 42 individuals across 12 macaque species. Columns represent the collection centers: CdP (Centre de Primatologie de l'Université de Strasbourg, France), Utrecht University (Netherlands), INSERM-Oxford University (Fr/UK), and Japan Monkey Center (Japan). Each row corresponds to a macaque species, with the number of individuals collected from each center. The total count per species and per center is indicated in the final column and row, respectively. The social grade of the species is indicated between brackets.

Document S1: Detailed brain extraction procedure

The first part of the acquisition of brain MRI images relies on the extraction of brain specimens. All the required materials are listed in **Table S1** and have been curated through literature recommendations (Brown et al., 2009; Davenport et al., 2014; King et al., 2013; Shatil et al., 2016) as well as through the realization of the procedure itself.

Table S2: Necessary materials for NHP brain extraction– name and description.

Materials	Description
Multifunctional rotary tool (Dremel type) associated with a sawing disc	To precisely cut out and remove the skull and have access to the brain.
Osteotome	To separate the skull from the atlas.
Mallet	Used with the osteotome.
Hammer-axe	To separate the skull from the atlas and to enlarge the space between the muscular planes and the skull.
Autopsy knife	To cut out the flesh and muscles.
Scalpel handle and blade	To dissect the scalp, muscles of the head, the dura, and the facial nerves.
Grooved probe	To dissect the dura without damaging the underlying tissues.
Pair of curved scissors with round tip	To cut out flesh at various steps of the dissection.
Dissecting forceps with and without claws	To hold tissues without damaging them to perform sections (skin, muscles, dura, nerves).
Graded beakers	To measure and transfer formaldehyde into the bucket for the brain fixation.
Funnel	To transfer the various liquids without spilling.
Test tube with graduation	To measure out the required amount of distilled water for the PBS.
Buckets (x4)	Containers for the brain fixation.
Hemispheric receptacles	With holes at regular intervals, to hold the brain spherical shape whilst it is immersed in formaldehyde.
Plastic jar with screw lid	Transparent, 7 centimeters in diameter (adapted to the size of the MRI antenna used). Container for brain during MRI acquisitions.

Fluorinert™ FC-770	Fluorocarbon-based fluid, helps to displace air bubbles[1] and improves brain/background image delineation.
Distilled water	To dissolve the PBS tabs to make PBS solution.
Parafilm	To seal the MRI containers and prevent any leakage.
Cotton batting/aquarium foam squares	To place inside the MRI container at the bottom, the top and on one side. Used to pad the brain specimen and contain the bubble at the top of the container.
FFP2 mask	Safety measures for zoonosis.
Latex or nitril surgical gloves	For handling specimen brains.
Lab coats (or surgical gowns)	For individual protection whilst performing the dissection.
Marker	To label the various containers (mentioning if it has contained formaldehyde), label the brain specimen.
7T MRI Antenna	For the MRI acquisition (whole brain acquisition). Check the internal diameter to choose the adequate container.
Material for the use of paraformaldehyde	
Formaldehyde solution 4 %	pH 6,9 solution for histological tissue fixation. Ordered from Sigma-Aldrich (Product ID: HT501640-19L).] At least 10 x volume of a macaque brain (roughly 3 liters per brain).
Formaldehyde spill response kits	Used for safety in case of any formaldehyde spilling.
Fume hood	To manipulate formaldehyde ensuring the safety of the experimenter.
Face shield	For the experimenter's safety in case of any spilling.
Mask	For the experimenter's safety in case of any spilling.
Gloves (chemical resistant)	For the experimenter's safety for handling the formaldehyde.
Baritainer	For discarding waste

[1] (Iglesias et al., 2018)

Summary table of the tools required for the brain extraction we performed, including their names and descriptions.

As it was the first time at the CdP that brain specimens were extracted, the development of a refined brain extraction technique played a central role in optimizing the quality of the acquired brain images. This technique, based on the literature, was meticulously applied to 17 *post-mortem* anatomical and DTI (if the specimen was not frozen) MRI scans. We optimally prepared through familiarizing with the technique and handling instruments such as the oscillating saw with a first brain extraction of a poor conditioned brain specimen (bad freezing condition). Through this first trial, we were able to adjust the following procedure as well as the chosen cutting landmarks. The brain extraction sequence consists of the following steps:

Head Dislocation: The animal is in supine position, with its head pulled dorsally to extend the neck (Brown et al., 2009). Then, the muscle mass of the neck has to be removed to expose the atlantooccipital junction. The junction is then incised, employing a back-and-forth motion to enable the passage of a knife or hammer-axis between the cartilage (Brown et al., 2009).

Adjustment for Frozen Specimens: For frozen specimens, a distinct approach through the atlantooccipital junction must be adopted. The section is performed with an osteotome and hammer **(Figure S1, A)**. Subsequently, confirmation of the absence of cerebellar protrusion through the foramen magnum is required and essential for ensuring the integrity of the specimens. If not, it would indicate cerebellar herniation and the presence of associated lesions in this brain structure (Davenport et al., 2014).

The head circumference was measured using a measuring tape during data collection. The average circumference of a macaque brain in our dataset is 30.5 ± 8.7 cm. We determined the amount of formaldehyde required based on the average volume of a macaque brain. This average volume is of 89.2 ± 1.9 (SEM) for male individuals and of 70.8 ± 0.72 cm^3 for female individuals (Franklin et al., 2000; Scott et al., 2016). The amount of 4 % formaldehyde buffered solution (pH = 6.9, Sigma-Aldrich) required to fix the brain should follow the volume ratio of tissue to be fixed to formaldehyde of 1:10 (Thavarajah et al., 2012), that is, a minimum of one liter of formaldehyde.

Skull Cap Removal: The removal of the skull cap is the most meticulous part of the procedure aimed at providing access to the brain. This process starts with a longitudinal incision of the scalp from the anterior fontanel cranial suture to the foramen magnum. A second incision is made perpendicular to the first, along the coronal suture. The exposed skull surface underwent thorough cleaning with 70% ethanol, followed by drying with gauze pads. The bony skull cap was then delicately excised using a rotary tool **(Figure S1. B)**.

Brain Extraction: The extraction of the brain from the skull was conducted with care especially for fresh specimens as the tissues are very soft and breakable. Removal of the dura mater, cerebellum tent, and false brain is performed using a bony cap (Brown et al., 2009). Afterwards, the head is positioned vertically and some gentle taps on the table to facilitate the gradual detachment of the brain from the skull. Employing a fluted probe, the olfactory

852 peduncles, internal carotid arteries, and cranial nerves are delicately severed (King et al.,
853 2013). The pineal gland is commonly found as a single white firm conical mass suspended at
854 the midline of the skull cap and attached to the meninges (King et al., 2013). In addition, in
855 many animals, the choroid plexus is visible as two reddish masses in a position similar to or
856 slightly in front of the pineal gland (King et al., 2013). Once the brain is fully extracted, it is
857 placed in one of the hemispheric cups. Frozen specimens are thawed in water at room
858 temperature before placing them in the cup (frozen tissue combined with formaldehyde fixation
859 creates an aqueous insulating layer, altering fixation of the internal brain structures) **(Figure**
860 **S1. D)**.

861 ***Fixation and Brain Preparation for MRI***

862 The fixation and preparation of brain specimens for MRI acquisitions is a crucial phase to
863 ensure high quality images and low prevalence of artefacts. The chosen fixative was a 10 %
864 formaldehyde buffered solution. Ensuring complete immersion of the brain in the fixative is
865 crucial. To achieve this, a carefully calculated volume of the solution is added to a labelled
866 container (usually around 3L). The brain is then placed within the container, submerged to
867 guarantee full coverage. Sealing the container prevents contamination. The container remains
868 for 7 days under the fume hood, and we check and gently stir every day to ensure the good
869 repartition of the formaldehyde on the tissue. Once the brain is fixed, it is immersed the brain
870 in a 0.5 L jar filled with PBS for 48 hours before MRI.

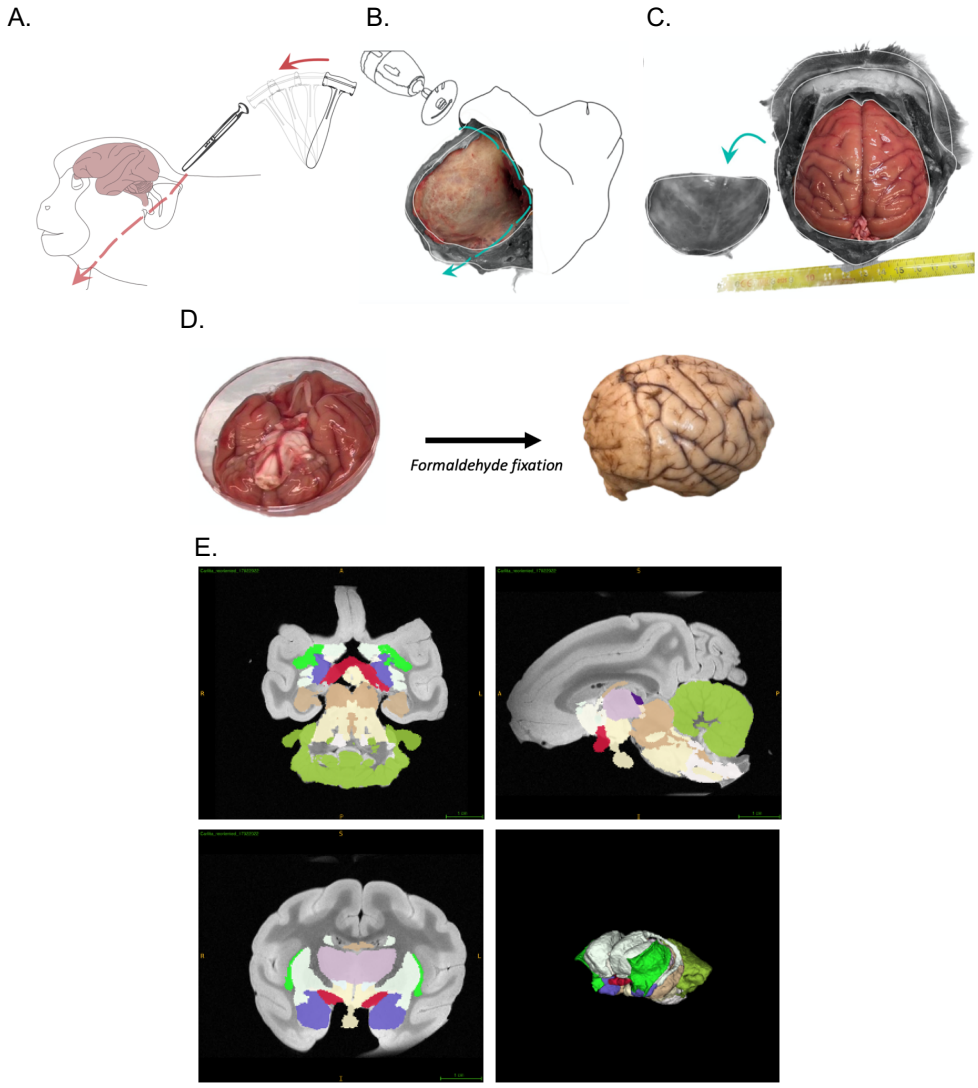

Figure S1: Sequence of dissection steps and MRI acquisition. *(A) Craniotomy step: Position of the cadaver and cut site. (B) Steps of scalp and skull removal using a Dremel tool® associated with a flex shaft rotary tool. (C) View of the skull after skull and dura removal. (D) Extraction and formaldehyde fixation of the brain. Right lateral view of the brain after a 7 day-formaldehyde-fixation. (E) SARM Regions (SARM2) and 3D MRI acquisition with atlas (bottom right). Amygdala (purple) (Hartig et al., 2021).*

1. MRI acquisitions

The diameter of the plastic container was chosen based on the diameter of the MRI antenna used (8,6 cm in diameter).

· The sample is placed in a spherical container. The orientation in which the brain is placed (for future reference during the MRI acquisitions) was registered. Aquarium foam squares are placed around the brain to minimize the residual movements from the MRI's vibrations and to contain the remaining air bubble at the top of the container (**Figure S2. B**).

· The container is filled to the brim with Fluorinert™ FC-770, a liquid that optimizes the contrast of the MRI signal and allows the wobble adjustment.

· The container is placed in a vacuum chamber (negative pressure of -0,1 Pa.), to limit the presence of air bubbles on the images, for up to three hours to remove air bubbles (Shatil et al., 2016) (**Figure 1, A**). If needed, some Fluorinert™ FC-770 can be added up to the brim.

· The container is sealed with parafilm (**Figure S2. B**).

2. Recommended 7T-MRI scanning setup

Place the container with an elevating foam square to contain the remaining bubble at the top of the jar and limit the superimposition of the bubble on the brain (**Figure S2. C and D**).

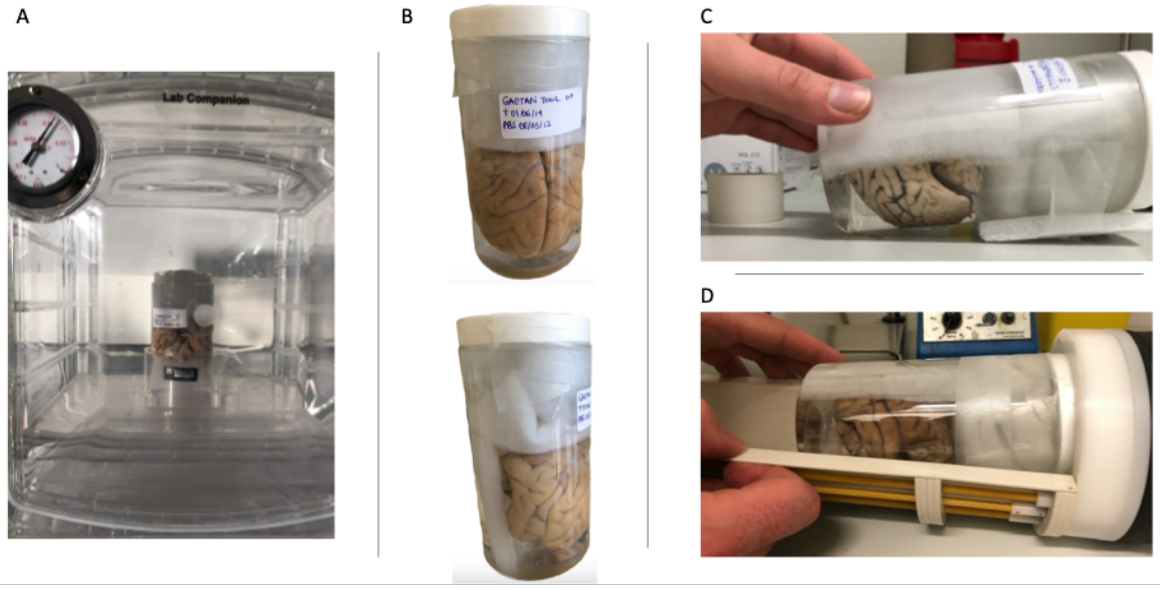

Figure S2: Set of photographs of the preparation of the fixed brain for MRI acquisitions. *(A) Air bubble removal stages in a vacuum chamber. The brain is immersed in Fluorinert™ FC-770 and held in position by the aquarium foam squares. The container is placed in a receptacle to catch any Fluorinert™ FC-770 that may spill out of the container during the procedure; (B) Placement of the aquarium foam squares inside the container of brain immersed in Fluorinert™ FC-770 and sealed with parafilm; (C) Placement of the container with a lift foam square to contain the residual air bubble in the top third of the container; (D) Placement of the container in the MRI antenna.*

Once in the MRI, it is recommended to perform a sequence of localizer scans with the purpose of: (1) identifying significant distortions caused by air bubbles in the brain or MRI-compatible container, (2) accurately positioning the brain, and (3) establishing the slice positions necessary for subsequent data acquisition (Shatil et al., 2016).

908 ***Table S3: Information relating to the acquisition of anatomical MRI images and the***
909 ***procedures for fixing and preserving post-mortem samples according to the different***
910 ***centers.***

MRI Center	Primatology Center (with ICube laboratory)	Utrecht University	Japan Monkey Center	Oxford University
Number of individuals	19	14	4	4
MRI	Bruker Biospec 7T 70/30 UR	Agilent Variant 9.4T	Bruker Biospec 9.4T 90/20 UR	Clinical Horizontal 3T
Antenna	Volume coil	Surface coil	Volume coil	Volume coil
MRI weighting	T2 Sequence: Turbo_RARE_3D	T1	T2	T2
Spatial resolution	0.20 x 0.20 x 0.20 mm	0.25 x 0.25 x 0.25 mm	0.25 x 0.25 x 0.25 mm	0.6 x 0.6 x 0.6 mm
Brain fixation characteristics	Immersion: Formaldehyde 4%	Perfusion: Formaldehyde 4%	Immersion: formaline 10%	Perfusion: Formaldehyde 4%
Fluid used for scanning	Fluorinert® FC-770	Sucrose 15%, 4°C	3M™ Fluorinert	Fomblin or Fluorinert® FC-770

911 Summary table of the MRI acquisitions parameters and *post-mortem* sample preservation
912 protocols across centers.

Supplementary references

Brown C, Rech RR, Torres F. 2009. A Field Manual for Collection of Specimens to Enhance Diagnosis of Animal Diseases. Boca Raton, FL, USA: Boca Publications Group, Incorporated.

Davenport AT, Grant KA, Szeliga KT, Friedman DP, Daunais JB. 2014. Standardized Method for the Harvest of Nonhuman Primate Tissue Optimized for Multiple Modes of Analyses. *Cell Tissue Bank* **15**:99–110. doi:10.1007/s10561-013-9380-2

Franklin MS, Kraemer GW, Shelton SE, Baker E, Kalin NH, Uno H. 2000. Gender differences in brain volume and size of corpus callosum and amygdala of rhesus monkey measured from MRI images. *Brain Res* **852**:263–267. doi:10.1016/s0006-8993(99)02093-4

Hartig R, Glen D, Jung B, Logothetis NK, Paxinos G, Garza-Villarreal EA, Messinger A, Evrard HC. 2021. The Subcortical Atlas of the Rhesus Macaque (SARM) for neuroimaging. *NeuroImage* **235**:117996. doi:10.1016/j.neuroimage.2021.117996

Iglesias JE, Crampsie S, Strand C, Tachrount M, Thomas DL, Holton JL. 2018. Effect of Fluorinert on the Histological Properties of Formalin-Fixed Human Brain Tissue. *J Neuropathol Exp Neurol* **77**:1085–1090. doi:10.1093/jnen/nly098

King JM, Roth-Johnson L, Dodd DC, Newsom ME. 2013. The Necropsy Book: A Guide for Veterinary Students, Residents, Clinicians, Pathologists and Biological Researchers, 7th ed. Cornell University, Ithaca, New York, 14850: College of Veterinary Medicine.

Scott JA, Grayson D, Fletcher E, Lee A, Bauman MD, Schumann CM, Buonocore MH, Amaral DG. 2016. Longitudinal analysis of the developing rhesus monkey brain using magnetic resonance imaging: birth to adulthood. *Brain Struct Funct* **221**:2847–2871. doi:10.1007/s00429-015-1076-x

Shatil AS, Matsuda KM, Figley CR. 2016. A Method for Whole Brain Ex Vivo Magnetic Resonance Imaging with Minimal Susceptibility Artifacts. *Frontiers in Neurology* **7**.

Thavarajah R, Mudimbaimannar VK, Elizabeth J, Rao UK, Ranganathan K. 2012. Chemical and physical basics of routine formaldehyde fixation. *J Oral Maxillofac Pathol* **16**:400–405. doi:10.4103/0973-029X.102496